Aus dem Zentrum für Augenheilkunde
der Universität zu Köln
Direktor: Universitätsprofessor Dr. med. C. Cursiefen

Hydrogen Sulfide: A Potential Therapeutic Treatment to Mitigate Pressure-induced Ferroptosis in Retinal Ganglion Cells

Inaugural-Dissertation zur Erlangung der Doktorwürde
der Medizinischen Fakultät
der Universität zu Köln

vorgelegt von
Yuan Feng
aus Heilongjiang, China

promoviert am 08.11.2024

Gedruckt mit Genehmigung der Medizinischen Fakultät der Universität zu Köln
Druckjahr: 2024

Dekan: Universitätsprofessor Dr. med. G. R. Fink

1. Gutachterin: Universitätsprofessorin Dr. med. V. Prokosch
2. Gutachter: Privatdozent Dr. med. R. Hörster

Erklärung

Ich erkläre hiermit, dass ich die vorliegende Dissertationsschrift ohne unzulässige Hilfe Dritter und ohne Benutzung anderer als der angegebenen Hilfsmittel angefertigt habe; die aus fremden Quellen direkt oder indirekt übernommenen Gedanken sind als solche kenntlich gemacht.

Bei der Auswahl und Auswertung des Materials sowie bei der Herstellung des Manuskriptes Unterstützungsleistungen von folgenden Personen erhalten:

Frau Prof. Verena Prokoch
Frau Dr. Hanhan Liu

Weitere Personen waren an der Erstellung der vorliegenden Arbeit nicht beteiligt. Insbesondere habe ich nicht die Hilfe einer Promotionsberaterin/eines Promotionsberaters in Anspruch genommen. Dritte haben von mir weder unmittelbar noch mittelbar geldwerte Leistungen für Arbeiten erhalten, die im Zusammenhang mit dem Inhalt der vorgelegten Dissertationsschrift stehen.

Die Dissertationsschrift wurde von mir bisher weder im Inland noch im Ausland in gleicher oder ähnlicher Form einer anderen Prüfungsbehörde vorgelegt. Einige der Ergebnisse dieser Arbeit wurden bei der Zeitschrift cell death and Disease eingereicht.

Die in dieser Arbeit angegebenen Experimente sind nach entsprechender Anleitung durch Frau Prof. Verena Prokoch und Frau Dr. Hanhan Liu von mir selbst ausgeführt worden. Die mtDNA-Mäuse wurden von der Arbeitsgruppe von Prof. Aleksandra Trifunovic und die NOX2-/- Mäuse von der Arbeitsgruppe von Dr. Marc Herb zur Verfügung gestellt.

Die Durchführung der Tierversuche wurde in Zusammenarbeit mit Frau Xiaosha Wang, Frau Panpan Li und der technischen Assistentin Rodica Maniu erfolgreich abgeschlossen. Die Probenvorbereitung für die Proteomik wurde gemeinsam mit Frau Xiaosha Wang durchgeführt, während die Analyse der Proben vom CECAD/CMMC Proteomics Core Facility durchgeführt wurde. Die Kultivierung der Netzhaut wurde in Zusammenarbeit mit Frau Panpan Li abgeschlossen. Alle anderen Experimente wurden unter der Anleitung der technischen Assistentin Rodica Maniu eigenständig von mir durchgeführt. Die Datenanalyse dieser Studie wurde unter der Leitung von Frau Hanhan Liu durchgeführt.

Erklärung zur guten wissenschaftlichen Praxis:

Ich erkläre hiermit, dass ich die Ordnung zur Sicherung guter wissenschaftlicher Praxis und zum Umgang mit wissenschaftlichem Fehlverhalten (Amtliche Mitteilung der Universität zu Köln AM 132/2020) der Universität zu Köln gelesen habe und verpflichte mich hiermit, die dort genannten Vorgaben bei allen wissenschaftlichen Tätigkeiten zu beachten und umzusetzen.

Köln, den

Unterschrift: ....

Acknowledgments

First and foremost, I would like to express my heartfelt gratitude to my supervisor, Univ-Prof. Dr. med. Verena Prokoch. I am deeply thankful for her guidance and support throughout the entire research process. She is not just my supervisor, but also my role model and mentor. Her passion for academia and life has profoundly influenced me, empowering me to tread the path of research with unwavering determination.

I am also immensely grateful to Dr. med. Hanhan Liu. As one of the main supervisors of my PhD project, she has provided me with meticulous academic guidance and selfless care in life. Each interaction with her brings fresh insights, and her unique perspectives always enlighten me. Her unwavering support and encouragement have given me the courage to confront the challenges in my work.

I want to sincerely thank my laboratory colleagues, who have been the most delightful companions. Special mention goes to Mr. Maoren Wang, Ms. Panpan Li, Mr. Xin Shi, Ms. Xiaosha Wang, Ms. Julia Prinz, Ms. Leila Frühn, Ms. Tienan Qi, and Ms. Rodica Maniu. Working with you has not only enriched my knowledge but also brought me much joy and friendship. Every moment we shared in the lab is a precious memory to cherish.

Moreover, I would like to express my heartfelt appreciation to friends who have offered assistance and support in life, including Ms. Huilin Yang, Ms. Jing Zhang, Ms. Sitong Ju, Ms. Xueting Li, Ms. Xiaojun Ju, Ms. Xincen Hou, Mr. Wanlin Fan, Ms. Yuqing Zhu, and Mr. Feng Ju. Your companionship and support have made my life in Germany vibrant and colorful. I am also grateful to every roommate I have lived with for your understanding and kindness, which have made me feel the warmth of home.

I want to offer a special thank you to my friends in China, whose frequent chats and comforting words have been my greatest solace in a foreign land.

Lastly, I want to deeply thank my parents. I love you both dearly. Thank you for always being my strongest support and loving me unconditionally. Your steadfast support is my driving force, and I will continue to strive to make you proud. And finally, I want to thank myself. Thank you for never giving up on pursuing a better self. I will always be proud of you!

Dedication

to my beloved YOU

CONTENTS

Abbreviations

RGCs	Retinal ganglion cells
IOP	Intraocular pressure
Fe^{2+}	Ferrous iron
Fe^{3+}	Ferric iron
GSH	Glutathione
GPx4	Glutathione peroxidase 4
NOX2	NADPH oxidase 2
H_2S	Hydrogen sulfide
ROS	Reactive oxygen species
CO_2	Carbon dioxide
GYY4137	Morpholin-4-ium-methoxyphenyl-morpholino-phosphinodithioate
Brn3a	Brain-specific homeobox/POU domain protein 3A
PFA	Paraformaldehyde
PBS	Phosphate buffer saline
DHE	Dihydroethidium
GO	Gene Ontology
KEGG	Kyoto Encyclopedia of Genes and Genomes
FE	Fold enrichment
TfR	Transferrin receptor
FTH1	Ferritin heavy chains
FTL	Ferritin light chains
GCL	Ganglion cell layer
IPL	Inner plexiform layer
INL	Inner nuclear layer
OPL	Outer plexiform layer
ONL	Outer nuclear layer

1. Zusammenfassung

Das Glaukom kann zum Tod retinaler Ganglienzellen (RGCs) und zu dauerhaften Sehbeeinträchtigungen führen. Ein erhöhter Augeninnendruck ist die Hauptursache für glaukomatöse Schäden. Allerdings verhindert allein die Kontrolle des Augeninnendrucks nicht vollständig den Verlust von RGCs beim Glaukom und die zugrunde liegenden Mechanismen bleiben unklar. In dieser Studie fanden wir heraus, dass Eisenstoffwechselstörungen, beeinträchtigte mitochondriale Funktionen und Ferroptose am Prozess der Drucksteigerung beteiligt waren, indem wir die Retina von Mäusen mit chronischer Druckerhöhung analysierten. Diese Faktoren könnten durch erhöhten Augeninnendruck auch am Schaden von RGCs beteiligt sein. In-vitro Studien bestätigten, dass eine chronische Druckerhöhung den Eisenimport förderte, den Eisenexport hemmte und zu einer abnormalen Anreicherung von zweiwertigem Eisen führte. Gleichzeitig führten mitochondriale Defekte auch zur Anreicherung von zweiwertigem Eisen und verursachten den Verlust von RGCs. Darüber hinaus führten mitochondriale Defekte und eine chronische Druckerhöhung zu einem erhöhten Spiegel reaktiver Sauerstoffspezies und erniederigten Glutathionspiegel. Eine chronische Druckerhöhung führte auch zur Erschöpfung der Glutathionperoxidase 4 (GPx4). Durch die Untersuchung von NADPH-Oxidase-2(NOX2) -Knockout-Mäusen stellte sich heraus, dass NOX2, im Vergleich zur Eisenstoffwechselstörungen, einer der effektiveren Auslöser, für die durch chronische Druckerhöhung verursachte GPx4-Reduktion war, was Ferroptose in RGCs weiter induzierte. Zusammenfassend ergab diese Studie, dass eine chronische Druckerhöhung Ferroptose in RGCs verursachte, indem sie Eisenstoffwechsel störte und mitochondriale Funktionen schädigte. Darüber hinaus zeigten wir, dass Schwefelwasserstoff eine eisenbindende und antioxidative Rolle zum Schutz von RGCs spielte, was eine Forschungsrichtung für das Verständnis und die Behandlung des Glaukoms darstellt.

Stichwörter: retinale Ganglienzellen, Eisenstoffwechsel, mitochondriale Funktion, Ferroptose, Schwefelwasserstoff, Glaukomtherapie

2. Summary

Glaucoma can lead to retinal ganglion cells (RGCs) death and permanent vision impairment. Elevated intraocular pressure (IOP) is the main cause of glaucomatous damage. However, only controlling IOP does not completely restrain RGCs loss in glaucoma, and the inner workings remain elusive. In this study, we found that iron metabolism disorders, impaired mitochondrial function, and ferroptosis participated in the pressure elevation by analysing the retinas of mice with chronic pressure elevation. Thus, these pathways may be involved in RGCs injury by elevated IOP. In vitro studies confirmed that chronic pressure elevation promoted iron import, inhibited iron export, and triggered the unusual deposition of ferrous iron (Fe^{2+}). At the same time, mitochondrial deficiency also caused an abnormal buildup ferrous iron and the loss of RGCs. In addition, chronic stress elevation and mitochondrial defects caused enhanced reactive oxygen species (ROS) levels and diminished glutathione (GSH) levels, and chronic stress elevation also caused glutathione peroxidase 4 (GPx4) exhaustion. By exploring NADPH oxidase 2 (NOX2) knockout mice, it was found that NOX2 was one of the more effective inducers of chronic pressure elevation induced GPx4 reduction compared to iron metabolism disorders, which further induced ferroptosis in RGCs. In conclusion, the present study revealed that chronic pressure elevation caused ferroptosis in RGCs by disrupting iron metabolism and damaging mitochondrial function. Furthermore, we demonstrated that hydrogen sulfide (H_2S) played an iron chelating and antioxidant role in the protection of RGCs, which provides a research direction for the understanding and treatment glaucoma.

Keywords: retinal ganglion cells, iron metabolism, mitochondrial function, ferroptosis, hydrogen sulfide, glaucoma therapy

3. Introduction

Glaucoma, with a global age-standardized prevalence estimated at 3-5% in individuals aged 40 years and older, is a significant contributor to permanent blindness affecting populations worldwide [1]. As the number and proportion of older people increase, the worldwide population of individuals suffering from glaucoma is anticipated to reach 111.8 million by 2040 [2]. Glaucoma comprises a spectrum of pathological conditions marked by the gradual deterioration of the optic nerve and concomitant decline in visual acuity. Such degeneration is primarily attributed to the irreversible demise of RGCs [3, 4]. Pathological IOP elevation is the most clinical manifestation of glaucoma, and it is also an essential factor in RGC death [5, 6].

3.1. Mechanisms of Pathological IOP Elevation Induced RGCs Death

The pathogenesis of glaucoma is very complex. Current research indicates that the potential mechanisms underlying RGCs death induced by elevated IOP primarily include: a. Mechanical compression of the optic disc and optic nerve due to increased pressure, resulting in axonal damage and interruption of transport, thereby impeding the transmission of neurotrophic substances to RGCs; b. Elevated pressure leads to a reduction in retinal blood flow, which induces ischemic injury to the RGCs; c. Accumulation of excitotoxic substances (such as glutamate and peroxides) due to increased pressure, thereby inducing RGCs apoptosis; d. Activation of immune responses, Inflammatory cell infiltration, resulting in damage to RGCs, and e. Other potential mechanisms [6-10].

Lowering IOP through pharmacological or surgical means remains the most effective therapeutic strategy for glaucoma [2, 11]. However, even with normalized IOP, many glaucoma patients experience ongoing deterioration of their visual fields [12]. Merely controlling IOP cannot fully prevent the progression of glaucoma [13, 14]. Pressure-induced RGCs death involves many other factors. Therefore, investigating and controlling these curative factors is very important to glaucoma treatment as well as improving the prognosis of glaucoma.

3.2. Association of iron homeostasis and ferroptosis with glaucoma

Iron, an essential trace element crucial for energy metabolism, growth, and development in the human body, is also indispensable for retinal function and metabolism [15, 16]. Epidemiological studies have consistently linked high iron intake and elevated serum ferritin levels to an increased incidence of glaucoma [17-19]. Our previous research has further illuminated the disruptive effect of significantly elevated IOP on retinal iron regulation [20].

Additionally, iron homeostasis emerges as a pivotal factor in optic nerve and RGCs [21, 22]. Collectively, these observations point to the vital role of iron metabolism in glaucoma and retinal degeneration. Iron-induced retinal damage is commonly attributed to ensuing mitochondrial dysfunction, excessive ROS production, and neuroinflammatory responses [23-25]. The concept of ferroptosis offers a novel perspective on glaucoma pathogenesis, emphasizing the intricate interplay with iron metabolism [26].

Ferroptosis represents a newly identified form of iron-dependent cell death, often accompanied by significant iron accumulation and lipid peroxidation during the process of cell death [26, 27]. Large intracellular iron accumulation, especially Fe^{2+}, generates large amounts of highly reactive hydroxyl radicals [26, 28]. They can oxidise lipid metabolites and form cytotoxic lipid peroxides [29]. At the same time, glutathione, which is used to scavenge lipid peroxides, is depleted and glutathione peroxidase activity is reduced, causing a decline in the antioxidant defenses of the cell allowing ROS to accumulate in the cell and promoting iron death [23, 29]. Numerous studies have demonstrated a connection between ferroptosis and glaucoma. It has been found that inhibition of ferroptosis increases the survival of RGCs in optic neuropathy [19, 30]. Our previous study of exogenous H_2S is tightly linked to pathways linked to the regulation of iron levels, ROS detoxification, and mitochondrial balance and activity, which are at the core of iron death [20]. This appears to provide a new direction for glaucoma drug therapy.

3.3. Protective role of H_2S

H_2S is regarded as a third endogenous signaling molecule comparable to carbon monoxide and nitric oxide [31]. Within a certain concentration range, H_2S plays crucial roles in the human nervous, vascular, and immune systems [32, 33]. Its sulphur ion can bind with free iron radicals, serving as an iron chelator to alleviate cellular damage from oxidative stress [34]. Additionally, research has shown that exogenous H_2S safeguards neuronal cells against glutamate-induced oxidative stress by enhancing the levels of the antioxidant glutathione [35, 36]. Moreover, research in certain cardiovascular and cerebrovascular diseases has revealed the ability of H_2S to dilate blood vessels, lower blood pressure, and improve circulation [37]. As its antioxidative, anti-inflammatory, and anti-apoptotic effects are gradually unveiled, H_2S demonstrates significant therapeutic potential in various neurodegenerative diseases within the central nervous system [23, 38-40].

A growing interest in recent years has been observed in studies exploring the link between H_2S and glaucoma. We have found that retinal endogenous H_2S synthase is altered by elevated IOP [41]. Moreover, an exogenous H_2S donor (GYY4137, a slow-release H_2S donor)

was effective in protecting RGCs from various glaucomatous injuries [41]. Although it has been shown in several studies that the neuroprotective effects of H_2S are partially attributed to its potential to induce vasodilation, attenuate oxidative stress, modulate neuroendocrine function, and inhibit inflammation, the exact underlying mechanisms remain unclear.

3.4. Purpose

Glaucoma, as the leading cause of global blindness besides cataracts, underscores the critical importance for glaucoma patients to explore pathogenesis and find preventive and therapeutic strategies. Pathological IOP elevation, the most important pathogenetic factor in glaucoma, appears to be interrelated with iron metabolism, mitochondrial function, and Ferroptosis. Nevertheless, emerging as a novel gas transmitter, H_2S also exhibits neuroprotective effects amidst pressure induced RGCs loss. Thus, this study aims to clarify the roles of iron and H_2S in pressure induced RGCs loss and iron death, crucially identifying (a) RGCs sensitivity to iron accumulation, (b) alterations in retinal iron content and regulation because of increased mechanical pressure contributing to ferroptosis, (c) which cellular signaling and events are in involved, and (d) potential therapeutic implications of H_2S in alleviating ferroptosis.

4. Material and Methods

4.1. Animal

Male C57BL/6 wild-type mice, aged 8-10 weeks (n=54), were used for this study. MtDNA mutator mice that were on a C57BL/6 background at the age of 37 weeks (n=3) were used to investigate the role of mitochondrial dysfunction. MtDNA mutator mice are genetically engineered mice harboring a transgenic mutation characterized by the expression of a proofreading-deficient variant of Polg A, the catalytic subunit of mitochondrial DNA (mtDNA) polymerase encoded by the nucleus [42]. MtDNA mutant mice were kindly provided by Prof. Aleksandra Trifunovic. $NOX^{-/-}$ ($gp91phox^{-/-}$) 8-9 week-old and wild-type (WT) mice (n=3) were used in the study. $NOX^{-/-}$ mice were graciously donated by Dr. Marc Herb.

All animals were housed in standard facilities provided by the Animal Faculty of University of Cologne Medical School. Adequate access to food and water was maintained ad libitum throughout a 12-hour day/night cycle. Ethical considerations regarding animal welfare were strictly adhered to. These ethical considerations followed the guidelines outlined in the German Animal Welfare Act. The guidelines also comply with European Community regulations and the ARVO ethical guidelines for the use of animals in ophthalmology and vision research. The guidelines involving animal experimentation conducted in this study underwent rigorous review and were approved by the competent regulatory authority overseeing animal rights regulations in North Rhine-Westphalia, Germany.

4.2. Chronic IOP Elevation Animal Model

Chronic IOP elevation in mice was induced in mice by cauterizing three external scleral veins, and the surgical method was specifically described in a previous study [41, 43]. Only the left eye was operated on, and the right eye was the control. The animals were continuously monitored for preoperative and postoperative IOP to ensure the stability of the animal model. Mice without sufficiently elevated IOP were excluded.

4.3. Preparation of Retinal Explants

Mouses were euthanized following carbon dioxide (CO_2) atmosphere. The surrounding tissues of the eye were immediately clipped with fiber scissors. The whole eyeballs were carefully put in phosphate buffer saline (PBS, Thermo Fisher, MA, USA). Separate the anterior segment of eyeballs under the microscope, preserving posterior segment of eye presented in the shape of a cup. Carefully dissect the complete retina. The retina was

equally divided into four flaps, as in the shape of a flower. The retina was positioned flat on filters (Millipore, Cork, Ireland), ensuring that the retinal ganglion cells were oriented upwards. The vitreous body left on the retinal surface was subsequently removed with forceps under the microscope.

4.4. Retina Culture

Retinal explants with filter paper were placed into tissue culture dishes (lumox dish, Nümbrecht, Germany). 8 quarters of retinal explants from different mice were assigned to one dish with 3ml culture medium. The culture medium consisted Dulbecco's Modified Eagle's Medium/Nutrient Mixture F-12 (Gibco BRL, Eggenstein, Germany) with an additional 10% Fetal Calf Serum (Biochrom, S0615) and 1% penicillin. Retina explants were incubated for 24 hours at 37°C in a humidified atmosphere with 5% CO_2 (Heracell 240i, Thermo Scientific, Germany).

The iron overload group was cultured with 500nM Hemin (51280, Sigma-Aldrich, Germany) for 1 hour as iron toxicity injury and then transferred to the regular culture medium for another 23 hours. Hemin can release two valence states (Fe^{2+} and ferric iron (Fe^{3+})), most of which are soluble and do not induce ferritin expression in most cells [44, 45]. It is widely used in various iron overload models [44-46]. We determined a concentration of 500 nM hemin to establish a retinal iron overload model based on the results of the pre-experiment (Supplementary Data S1 “Impact of Different Concentrations of Hemin on RGCs”).

The high-pressure group was cultured in the pressure-ready metallic incubation as mentioned in our previous study [41]. Retina explants were under fluctuating hydrostatic pressure in a pressure chamber for 6 hours and cultured under 0mmHg for another 18 hours. The pressure within the chamber was elevated to 60mmHg and subsequently reduced gradually to 0mmHg over a 15-minute cycle throughout the 6-hour culture period.

Morpholin-4-ium-methoxyphenyl-morpholino-phosphinodithioate (GYY4137) is an H_2S precursor that releases H_2S slowly and continuously in a similar way to protect endogenous H2S [47]. In our previous study, GYY4137 showed a protective effect on the retina at 100 nM [41]. Therefore, this concentration was selected as the culture condition for the H_2S group in this study. Retinal explants were cultured with 100nM GYY4137 (Sigma-Aldrich, Germany) for 24 hours. The culture conditions regarding pressure were the same as those of the high-pressure group.

4.5. Proteomics and Analysis

Quarters of the retinas from mice after episcleral vein cauterization were used for proteomic analysis. T-PER tissue protein extraction reagent (REF78510, thermos scientific, USA) with phosphatase inhibitors (P8340, sigma, USA) was used to lyse the retina. Centrifugation was performed at 10,000 rpm for 5 minutes, after which the supernatant was collected. Sample protein concentration in the sample was quantified via the BCA assay (WG327090, Thermo Scientific, USA). Proteomics samples were prepared according to the SP3 protocol [48]. Samples containing 20 μg protein concentration were measured by the CECAD/CMMC Proteomics Centre at the University of Cologne. A Q Exactive Plus tandem mass spectrometer (Thermo Scientific) was used to analyze the peptides [49]. Use the PANTHER (accessed on 17 September 2023) and STRING (accessed on 24 October 2023) online analysis tools to understand protein information and analyze the data.

4.6. RGCs Quantification

RGCs were validated through immunohistochemical staining targeting brain-specific homeobox/POU domain protein 3A (Brn3a) in retinal flat-mount [50]. Retinal explants were immersed in 4% paraformaldehyde (Karlsruhe, Germany) for 30 minutes, followed by incubation in a 30% sucrose solution at 4°C overnight. After washing with PBS, the explants were placed in 0.3% Triton X-100 in PBS (PBS-T) for 30 minutes. Subsequently, the samples were blocked with 1% skim milk PBS-T at room temperature for 30 minutes. Primary antibody (1:200, anti-Brn3a mouse monoclonal antibody, Germany) incubation was performed overnight at 4°C. After three washes with PBS-T, the samples were labeled using a secondary antibody (1:1000; goat anti-mouse IgG AlexaFluorTM488, Abcam) at room temperature for 1 hour in dark. Afterwards, samples were mounted on slides after washing three times with PBS. Fluorescent staining was observed under a fluorescence microscope (Axio Imager M2, Zeiss, Germany) at a magnification of 20x. Photographs were captured at six distinct regions of the retina within each quadrant. Quantification of Brn3a-positive cells was used ImageJ v2.3.0 software.

4.7. Immunofluorescence Staining

The retinal explants were placed into molds containing optimal cutting temperature (OCT) compound and frozen. Retinas were cut longitudinally with a cryostat (CM3050S, Leica, Germany) and their cross-sectional tissues (12 μM) were affixed to sections and air-dried naturally. After washing the retinal cryosections three times with PBS, the tissue on the slides was permeabilized in a blocking solution containing 1% bovine serum albumin (BSA) and 0.1% Triton X-100 at room temperature for 30 minutes. Primary antibody incubation was

performed on the cryo-sections for 2 hours. After that, the secondary antibody (1:1000, goat anti-rabbit IgG H + L Alexa Flour 546, CA, USA) incubated sampled for 1 hour away from light. The slides were mounted with mounting medium containing DAPI (BIOZOL, Germany) after washing with PBS. Refrigerated the slices at 4°C for 1 hour to make them seal better. The cryo-sections were scanned at 20x magnification using a confocal fluorescence microscope (Airy Scan Confocal, Zeiss). The same exposure parameters were set and twenty scans at the same intervals were selected. The images were stacked by the Z-stack function of the microscope to compose a single photograph. The fluorescence intensity in the composite photo was measured by ImageJ v2.3.0 software. Each retinal layer's fluorescence intensity was assessed separately.

Primary antibodies for staining the retinal cryo-sections were anti-ferritin light chain (ab69090, Abcam), anti-ferritin heavy chain (ab75973, Abcam), anti-transferrin receptor (ab84036, Abcam), and anti-Hepciden (ab190775, Abcam). All dilutions were 1:200 in blocking solution.

4.8. Iron Quantificationl

Iron content (total iron, Fe^{2+}, and Fe^{3+}) in the retina and the brain were quantified by an iron assay kit (MAK025, Sigma). Sample preparation and measurement methods followed the kit instructions. A spectrophotometric multi-well plate reader (TECAN infinite F200 Pro) determined the absorbance at 593 nm.

4.9. Western Blotting

Cultured retinal explants and mouse brain tissue were homogenized and lysed in cold T-PER buffer containing protease inhibitors. The samples were centrifuged at 10,000 rpm for 10 minutes at 4°C, and the supernatant was collected. Protein concentration was determined using a BCA protein assay kit. A total of 15 µg of protein was mixed with 4x sample buffer and denatured by boiling at 98°C for 5 minutes. The protein samples and molecular weight markers were loaded onto a sodium dodecyl sulfate-polyacrylamide gel (SDS-PAGE) and separated at 130 V. The separated proteins were transferred from the gel onto a polyvinylidene fluoride membrane (PVDF, 1704157, bio-red). Following a one-hour blocking step at room temperature with 5% skim milk. The membrane was then incubated overnight at 4°C with primary antibodies on a shaker. The primary antibodies used were: anti-GPX4 (1:1000, ab125066, Abcam), anti-NOX2 (1:1000, ab129068, Abcam), anti-beta-actin (1:4000, ab6276, Abcam). After washing the membrane with TBS-T, it was incubated with the appropriate secondary antibody (1:4000; Sigma-Aldrich) for 1 hour. After a brief wash with PBS, chemiluminescent solution (Millipore, Bedford, MA) was evenly mixed and applied to

the membrane for 2 minutes. The protein blots on the membrane were detected using an automated chemiluminescence analysis system (Millipore, Billerica, USA). Protein band intensities were analyzed for optical density using ImageJv2.3.0 software.

4.10. Quantification of Oxidative Stress

GSH is an important biochemical indicator of oxidative stress [51]. GSH Assay Kit (ab239727, Abcam) was used to measure the level of GSH in retina and brain. Measurement methods followed the kit instructions. Dihydroethidium (DHE) fluorescent staining was used to indirectly quantify ROS levels in retina. 12 μm-thickness retinal cryo-sections were stained with DHE (1μM) as reported previously [52]. The fluorescence intensity of DHE was quantified by the method of photography and measurement described in the immunofluorescence staining.

4.11. Statistic Analysis

The data presented in this study were derived from distinct biological samples. The sample sizes were determined according to established protocols in the field, ensuring statistical power and consistency across experiments. Each experiment was repeated with a minimum of three independent biological replicates to ensure the reliability and reproducibility of the results. Statistical analyses and graphical representations were conducted using GraphPad Prism software (version 9.2, San Diego, California, USA). Data are expressed as the mean ± standard error of the mean (SEM), with "n" representing the number of biological samples per group. To compare two groups, unpaired Student's t-test was employed, while for multiple group comparisons, one-way analysis of variance (ANOVA), followed by Tukey's post hoc test, was applied to identify specific differences between groups. These statistical methods were chosen to account for both within-group variability and between-group comparisons. Prior to performing these tests, the assumption of sample independence, normal distribution of data, and equality of variances was thoroughly checked using standard diagnostic tools. A significance threshold of $P < 0.05$ was validated as statistically significant.

5. Result

5.1. The Altered Abundance of Proteins Associated with Iron Metabolism and/or Mitochondrial Function was Outstanding in Chronic IOP Elevation.

To investigate which proteins were associated with retinal damage under chronic high pressure. We collected retinas from mice with elevated IOP after external scleral vein cauterization for proteomics based on mass spectrometry. A total of 5754 proteins were identified by proteomics. Chronically elevated IOP resulted in a marked reduction in the expression of 54 proteins and a substantial increase in the expression of 506 proteins (Figure 1A). Based on the PANTHER gene classification analysis, 21 proteins were categorized as either mitochondrial proteins or proteins associated with iron metabolism (Table 1). Twelve of these proteins showed a significantly increased abundance due to chronic IOP elevation. Whereas nine proteins showed a significant decrease in abundance (Table 1). Figures 1B and 1C showed the 10 proteins with the most significant increase/decrease in protein abundance due to chronic pressure elevation, respectively.

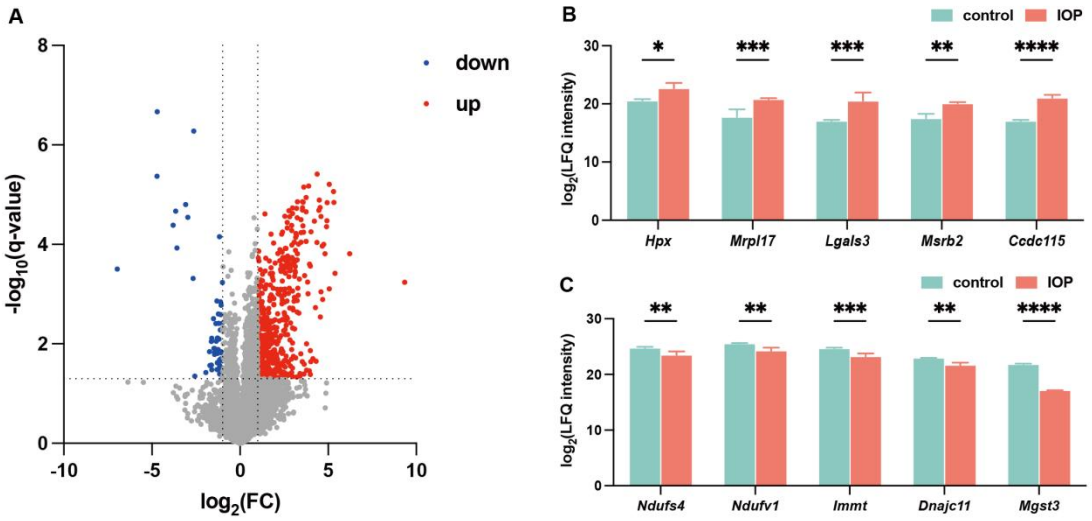

Figure 1 *(A) The volcano plot displayed proteins with differential expression between the chronic IOP and control groups. The X-axis represents the fold change in LFQ Intensity between groups, while the Y-axis represents the statistical significance (-1 × log10(p-value)) for each protein. Red dots signify up-regulated proteins, blue dots signify down-regulated proteins. (B-C) Changes in the expression of five up-regulated proteins and five down-regulated proteins associated with mitochondrial and/or iron metabolism most affected by chronic IOP elevation.*

Table 1 List of 21 Significantly Differentially Expressed Retinal Proteins Identified in the IOP Group.

Protein IDs	Gene Names	Protein.Description	q-Value	Fold change
Q8VE99	Ccdc115	Mitochondrial import receptor subunit TOM40 homolog	0.0478125	3.9932
P16110	Lgals3	MICOS complex subunit Mic60	0.0439209	3.45037
Q9D8P4	Mrpl17	Hemoglobin subunit alpha	0.0407034	3.04772
Q78J03	Msrb2	Microsomal glutathione S-transferase 3	0.0490746	2.57809
Q91X72	Hpx	Glutathione S-transferase P 1	0.0385444	2.12963
P01942	Hba	Mitochondrial import receptor subunit TOM40B	0.0485911	1.83171
Q8BUE4	Aifm2	Ferroptosis suppressor protein 1	0.0374941	1.78971
Q8VCF0	Mavs	DnaJ homolog subfamily C member 11	0.0453551	1.45094
P10649	Gstm1	Coiled-coil domain-containing protein 115	0.0409536	1.39597
Q8BGS2	Bola2	NFU1 iron-sulfur cluster scaffold homolog, mitochondrial	0.040939	1.30064
P19157	Gstp1	39S ribosomal protein L17, mitochondrial	0.0381269	1.06525
Q9QZ23	Nfu1	NADH-ubiquinone oxidoreductase 75 kDa subunit, mitochondrial	0.0414184	1.04723
Q9QYA2	Tomm40	NADH dehydrogenase [ubiquinone] flavoprotein 1, mitochondrial	0.0418638	-1.07055
Q9DC70	Ndufs7	BolA-like protein 2	0.0369699	-1.09597
Q9CZR3	Tomm40l	NADH dehydrogenase [ubiquinone] iron-sulfur protein 7, mitochondrial	0.0432374	-1.10691
Q91VD9	Ndufs1	Methionine-R-sulfoxide reductase B2, mitochondrial	0.038689	-1.16232
Q5U458	Dnajc11	Mitochondrial antiviral-signaling protein	0.0388718	-1.27489
Q91YT0	Ndufv1	Hemopexin	0.0377527	-1.28226
Q9CXZ1	Ndufs4	NADH dehydrogenase [ubiquinone] iron-sulfur protein 4, mitochondrial	0.0413944	-1.28254
Q8CAQ8	Immt	Galectin-3	0.0386595	-1.44686
Q9CPU4	Mgst3	Glutathione S-transferase Mu 1	0.0369687	-4.69653

5.2. Involvement of Pathways Related to Ferroptosis and Mitochondrial Function in Retinal Impairment Induced by Chronic IOP Elevation.

To investigate which pathways were regulated differentially with chronic IOP elevation, we further performed Gene Ontology (GO) and Kyoto Encyclopedia of Genes and Genomes (KEGG) analyses based on mass spectrometry results.

According to GO, the biological processes of "regulation of translation", "protein transport", "aerobic respiration," and other biological processes were influenced by chronic IOP elevation. Among them, "protein transport" was even enriched with 35 genes (Figure 2A). The cellular components were mainly distributed in "macromolecular complex", "respiratory chain", and "mitochondrial respiratory chain complex I". 47 genes were closely associated with "macromolecular complexes" (Figure 2B). During chronic IOP elevation, significant molecular functions included "macromolecular complex binding," "protein kinase binding," "NADH dehydrogenase (ubiquinone) activity," among others. Notably, "metal ion binding" exhibited enrichment with up to 118 genes (Figure 2C). KEGG pathway analysis revealed three pathways with the highest fold enrichment (FE) metrics: "Ferroptosis" (FE=4.2257), "Chemical carcinogenesis - reactive oxygen species" (FE=3.8069), and "Parkinson's disease" (FE=3.5214). Additionally, the pathway with the most enriched proteins was "Pathways of neurodegeneration - multiple diseases" which exhibited enrichment of 37 relevant proteins (Figure 2D).

To observe the interaction relationships between target proteins, we uploaded a list of target proteins that had been analyzed according to the PANTHER Family/Subfamily classification to the STRING analysis. Proteins related to iron homeostasis, ferroptosis, and glutathione metabolism were strongly linked in the protein interaction network. Furthermore, proteins implicated in oxidative phosphorylation were enriched and interacted with GPx4 in the contexts of ferroptosis and iron homeostasis, as depicted in Figure 2E.

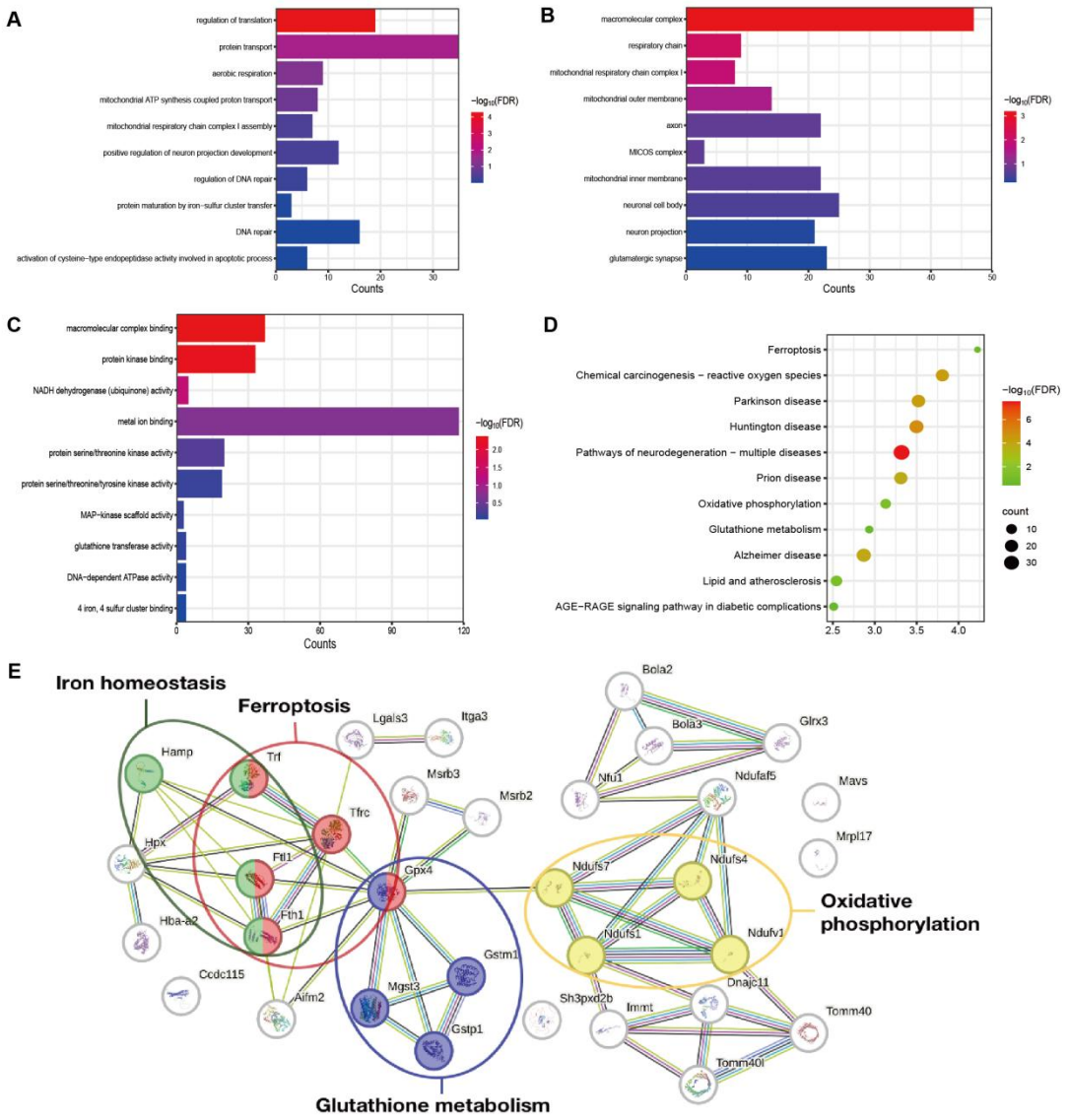

Figure 2 *(A-C) Bar plot displaying GO enrichment analysis results for differentially expressed proteins between the IOP and control groups. X-axis represents the quantity of enriched genes, while the Y-axis represents various GO terms (biological processes, cellular components, and molecular functions). Bars depicts -log10 FDR values. (D) Bubble plot of KEGG enrichment analysis for differentiated expressed proteins between the IOP and the control groups. X-axis represents ratios (number of differential proteins over total proteins). The size of the dots reflects the quantity of enriched genes. The color of the dots represents the value of -log10 FDR. (E) Network analysis graph of target protein interactions. Green nodes labeled proteins associated with iron homeostasis. Red nodes labeled proteins associated with ferroptosis. Blue nodes labeled proteins associated with glutathione metabolism. Yellow nodes labeled proteins associated with oxidative phosphorylation. The edges between the nodes represent the interaction relationship between the two proteins connected by the edge.*

5.3. Iron Overload, Elevated Hydrostatic Pressure, and Mitochondrial Mutation Led to RGCs Loss, and H_2S Protected RGCs from Elevated Hydrostatic Pressure Induced Injury.

To explore the impact of iron toxicity, high pressure, and mitochondrial mutations on RGCs, we counted the number of surviving RGCs. Both iron overload (1316±182.0 RGC/mm^2) and elevated hydrostatic pressure (1233±222.8 RGC/mm^2) significantly reduced RGCs survival compared to the control group. The RGCs of retinal explants cultured with H_2S precursors (1479±154.1 RGC/mm^2) increased by approximately 16% compared with the high pressure group, and did not differ significantly from those of the control group (1549±238.0 RGC/mm^2) (Figure 3A,B).

The number of RGCs was reduced by 31.24% in mtDNA mutator (2104±290.7 RGC/mm^2) compared with age-matched WT mice (3060±304.2 RGC/mm^2) (Figure 3C, D).

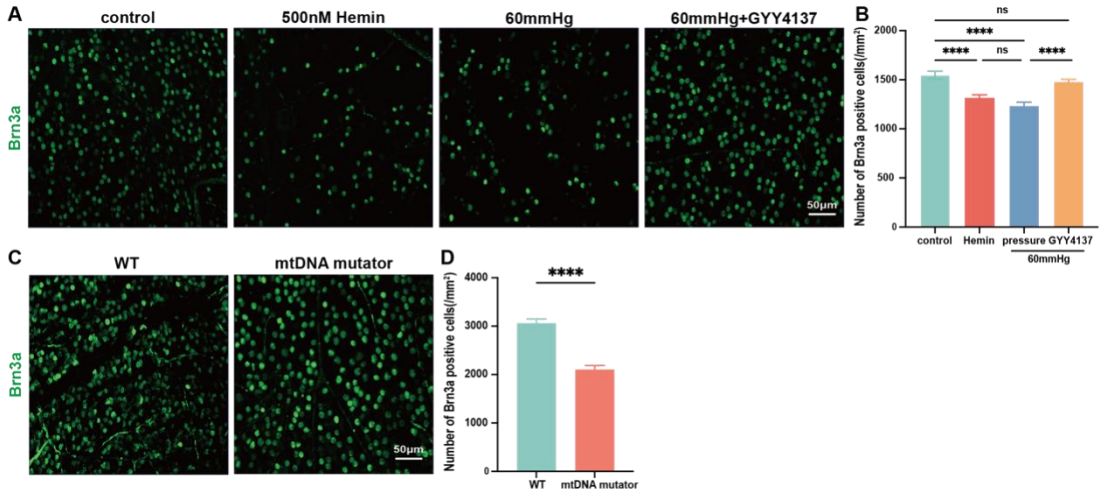

Figure 3 *(A, C) Typical fluorescence microscopy images of RGCs in different groups; (B, D) Statistical analysis of RGCs (Brn3a-positive cell counts) in the retina flat-mount. (ns: no significance; **** p<0.0001; scale bar = 50 μm)*

5.4. Iron Overload, Elevated Hydrostatic Pressure, and Mitochondrial Mutation Increased Iron Content. H_2S Attenuated High Pressure-Induced Iron Overload.

Iron content and composition were assessed in retinas exposed to iron overload and elevated hydrostatic pressure as well as in brain from mtDNA mutant mice. In in vitro retinal tissue cultures, both iron overload (p<0.01) and elevated hydrostatic pressure (p<0.001)

significantly increased the total iron and Fe^{2+} content (Figure 4A). The addition of the H_2S precursor reduced both total iron and Fe^{2+} content in retina, showing no significant distinction from the control group (Figure 4A). In the compositional analysis, the proportion of Fe^{2+} to total iron content was significantly higher than that of Fe^{3+}. The percentage of Fe^{2+} to total iron increased significantly under iron overload (94.5%) and high pressure (91.41%). However, after H_2S precursor treatment, the percentage of Fe^{2+} (89.97%) was nearly identical to the control (89.62%, Figure 4B).

In the brains of mtDNA mutators, total iron ($p<0.0001$) and Fe^{2+} content ($p<0.01$) was significantly increased over their age-matched WT mice (Figure 4C). The percentage of Fe^{2+} to total iron content was also significantly more than the percentage of Fe^{3+}. However, the percentage of Fe^{2+} in the brains of mtDNA mutators (73.18%) was lower than that of WT mice (85.9%, Figure 4D).

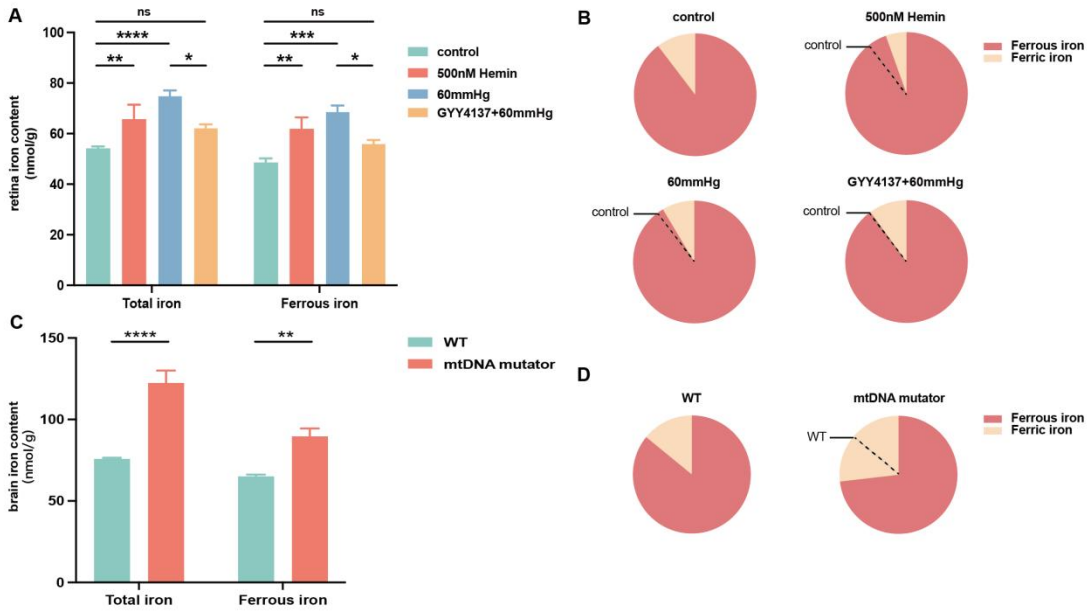

Figure 4 *(A) Quantification of retinal iron content under the different in vitro culture conditions; (B) Retinal iron composition; (C) Quantification of brain iron content in WT mice and mtDNA mutators. (D) Brain iron composition in WT mice and mtDNA mutators.*

5.5. Retinal Iron Homeostasis was Disrupted by Iron Overload and Elevated Hydrostatic Pressure. H_2S Attenuated Iron Disorders Induced by Elevated Hydrostatic Pressure.

To investigate how elevated hydrostatic pressure affected retinal iron homeostasis, we evaluated the localization and expression of four iron-regulated proteins that play critical roles in iron import, export, and storage in the retina.

The transferrin receptor (TfR) picked up transferrin complexes synthesized with extracellular non-heme iron and transferred extracellular iron into the cell via endocytosis [53]. Immunofluorescence staining of retinal cryo-sections revealed widespread expression of TfR throughout the retina, with notable concentrations in ganglion cell layer (GCL), inner plexiform layer (IPL), and inner nuclear layer (INL) (Figure 5A). Both iron toxicity and elevated hydrostatic pressure significantly elevated TfR fluorescence intensity in the retina ($p<0.0001$), particularly in the inner layers ($p<0.0001$). Despite exposure to elevated hydrostatic pressure, the fluorescence intensity of TfR was dramatically reduced ($p<0.0001$) with H_2S precursors treatment (Figure 5B-D).

Hepcidin binds to and degrades ferroportin, inhibiting cellular iron export and thereby regulating iron utilization and storage [54]. Our findings demonstrated widespread expression of hepcidin throughout all retinal layers (Figure 5E). Elevated hydrostatic pressure significantly increased hepcidin fluorescence intensity in the retina ($p<0.0001$), particularly in GCL and inner layer ($p<0.0001$, Figure 5F-H). No considerable changes were detected in iron overload. Treatment with H_2S precursor contributed to a notable decrease in hepcidin fluorescence intensity ($p<0.0001$), without any significant difference from the control group (Figure 5F-H).

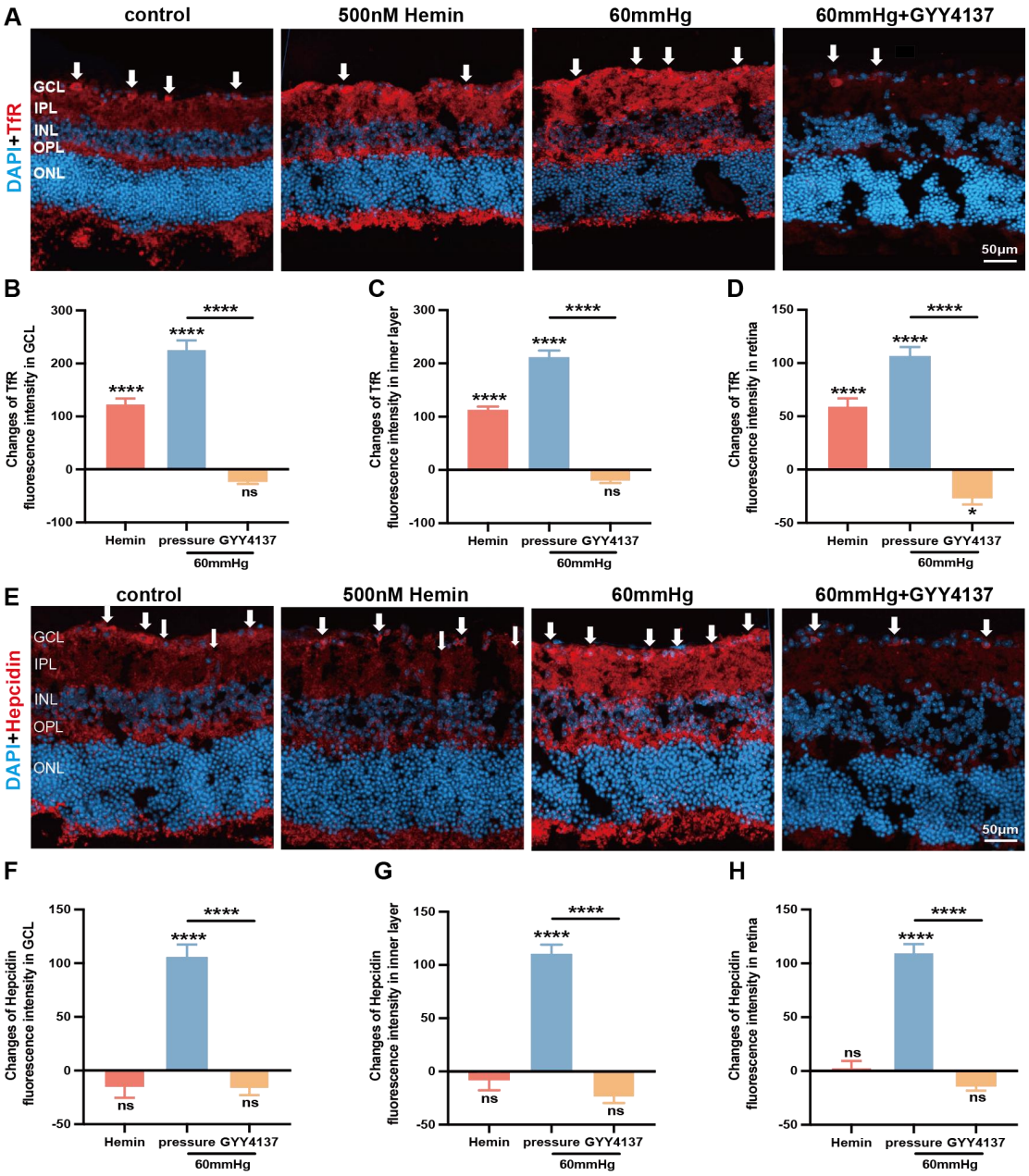

Figure 5 *(A, E) Representative microscopic photographs of TfR and Hepcidin immunofluorescence staining in retinal cryo-sections; (B-D, F-H) Changes in fluorescence intensity of TfR and Hepcidin GCL, inner layer and the whole retina. (GCL: ganglion cell layer; IPL: inner plexiform layer; INL: inner nuclear layer; OPL: outer plexiform layer; ONL: outer nuclear layer. Each group was compared with the control, scale bar = 50 μm).*

The ferritins are responsible for storing iron within cells in a stabilized form and are constituted of ferritin heavy chains (FTH1) and ferritin light chains (FTL) [53]. Like other iron regulatory proteins, both FTH1 and FTL were expressed across nearly every layer of the retina (Figure 6A, E).

Higher fluorescence intensity of FTH1 in the retina was observed in the elevated pressure group. However, statistically, neither iron overload nor elevated hydrostatic pressure induced significant changes in FTH1 fluorescence intensity. Treatment with H_2S precursor notably mitigated pressure-induced alterations in FTH1 expression, exhibiting no meaningful difference from the control group (Figure 6B-D).

The fluorescence intensity in retina of FTL did not significantly change under iron overload or elevated hydrostatic pressure (Figure 6F-H).

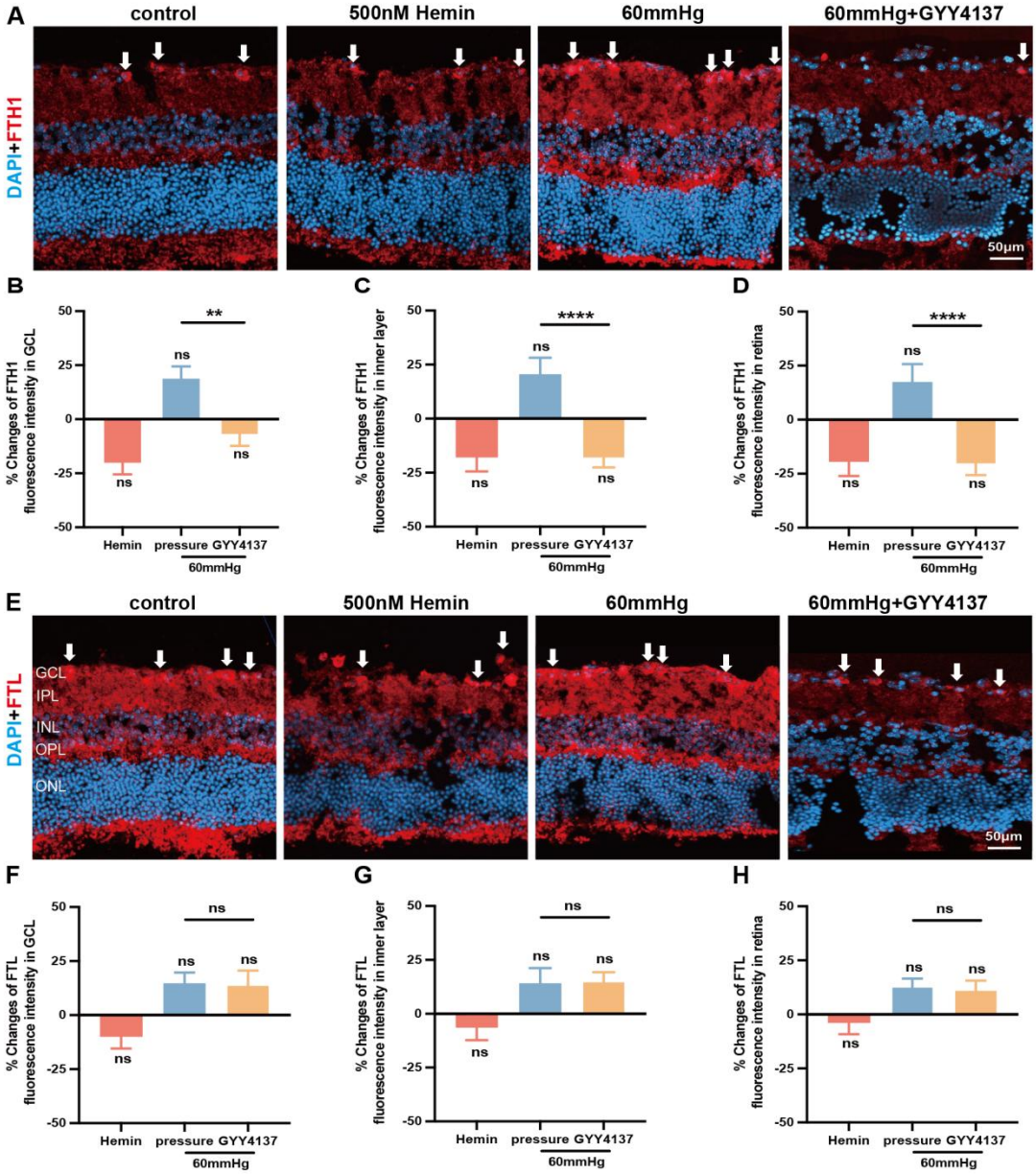

Figure 6 *(A, D) Representative microscopic photographs of FTH and FTL immunofluorescence staining in retinal cryo-sections. (B-D F-H) Changes in fluorescence*

intensity of FTH and FTL in GCL, inner layer and the whole retina. (Each group was compared to the control, scale bar = 50 μm).

5.6. Iron Overload and Elevated Hydrostatic Pressure Induced ROS and NOX2 NADPH Oxidase Alterations in the Retina. H_2S Effectively Mitigated the High Pressure-induced Alterations in ROS Levels and NOX2 Expression.

Fe^{2+} is considered a strong oxidant and its excessive accumulation exacerbates intracellular oxidative stress [55]. To investigate whether the accumulation of total iron and Fe^{2+} levels in the retina lead to an augmented oxidative stress, we employed the DHE fluorescent staining to measure ROS levels. In comparison to the control group, iron overload significantly increased the fluorescence intensity of DHE in GCL ($p<0.001$), with no significant alterations observed in the inner layer and the whole retina (Figure 7B-D). Elevated hydrostatic pressure increased the fluorescence intensity of DHE in the whole retina ($p<0.01$, Figure 7D). Changes were particularly noticeable in the inner layers, especially the GCL ($p<0.001$, Figure 7B, C). However, H_2S mitigated the pressure-induced elevation of DHE fluorescence intensity in retina, particularly evident in the GCL ($p<0.001$, Figure 7B-D).

The NOX2 NADPH oxidase plays a pivotal role in generating antimicrobial ROS [56]. Interestingly, under conditions of iron overload, there were no observable changes in the fluorescence intensity of NOX2, both within GCL and the whole retina. Conversely, Elevated hydrostatic pressure induced a substantial increase in NOX2 fluorescence intensity in the GCL, inner retina, and the whole retina ($p<0.05$, Figure 7F-H). Notably, the supplementation of H_2S precursor significantly attenuated the pressure-induced elevation in NOX2 fluorescence intensity (Figure 7F-H).

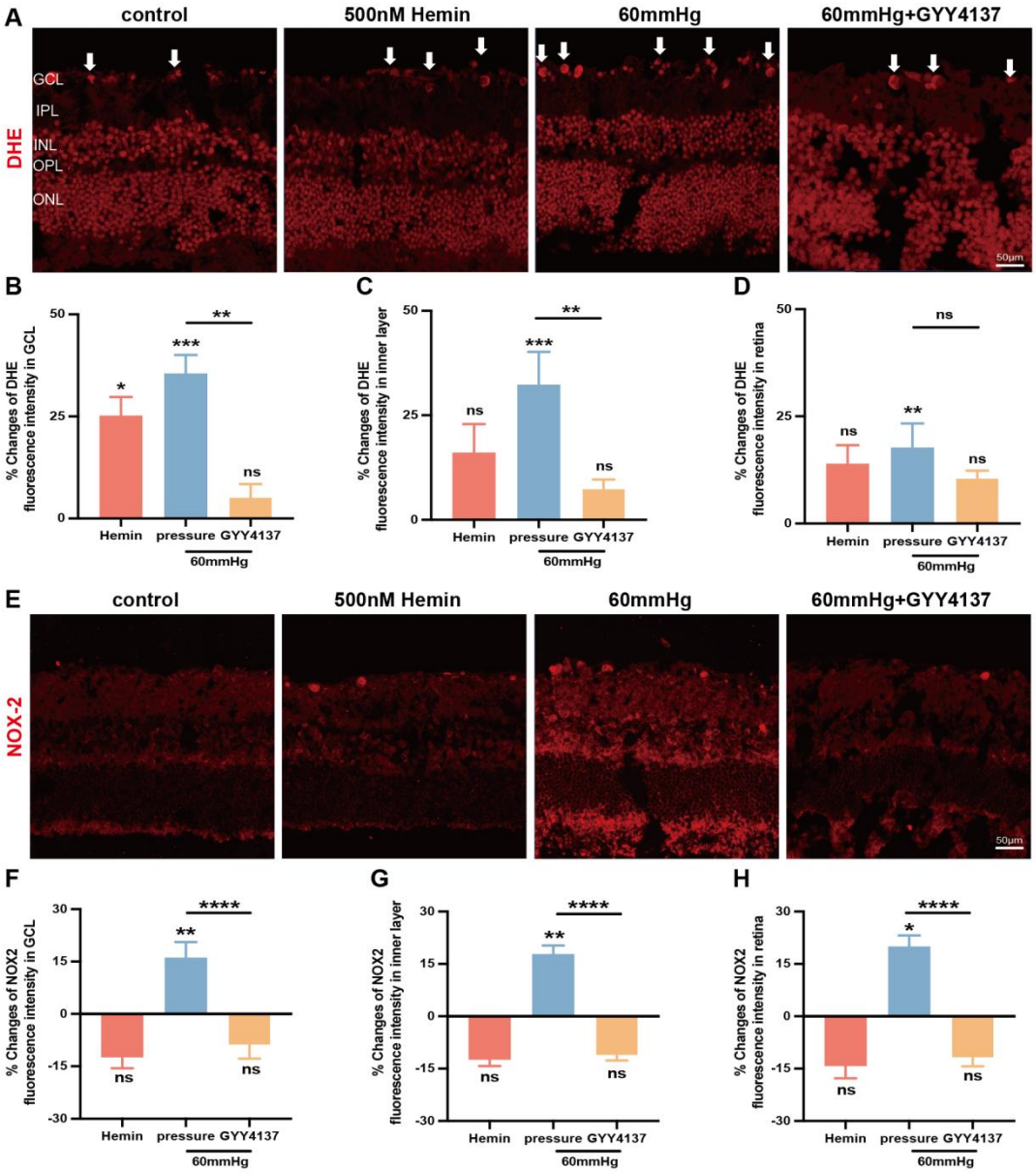

Figure 7 *(A, E) Representative fluorescence micrographs of DHE and NOX2 fluorescent staining in retinal cryo-sections; (B-D, F-H) Changes in fluorescence intensity of DHE and NOX2 in GCL, inner layer and the whole retina. (Each group was compared to the control, scale bar = 50 μm).*

5.7. Impact of Iron Overload, Elevated Hydrostatic Pressure, and Mitochondrial Mutation on Ferroptosis in the Retina. H_2S Attenuated Ferroptosis Induced by High Pressure.

Ferroptosis is iron-dependent regulatory cell death, where compromised activity or deficiency of GPx4, alongside increased availability of ferrous iron, culminates in ferroptosis triggered by lipid peroxidation [29, 57]. GSH and GPx4 are the building blocks of the antioxidant defense.

To investigate whether the antioxidant capacity of the retina is changed under iron overload, elevated hydrostatic pressure, and mitochondrial mutation, we measured GSH levels and GPx4 expression in the retina and brain. Both iron overload and elevated hydrostatic pressure induced a marked reduction in retinal GSH levels, as illustrated in Figure 8A. The H_2S precursor restored GSH levels and was not statistically different between the control (15.84 ± 1.87 nmol/mg) and H_2S group (13.66 ± 1.01 nmol/mg, Figure 8A). Additionally, a notable reduction in GSH levels was found in the brains of mtDNA mutator mice (63.93±13.66nmol/mg) compared to WT mice (86.08±6.48nmol/mg, $p<0.05$, Figure 8B).

Although iron overload and mitochondrial mutation exhibited negligible impact on GPx4 expression within the retina and brain, elevated hydrostatic pressure notably diminished GPx4 expression in the retina. However, H_2S precursors restored the reduced activity of GPx4 induced by elevated hydrostatic pressure (Figure 8C-F).

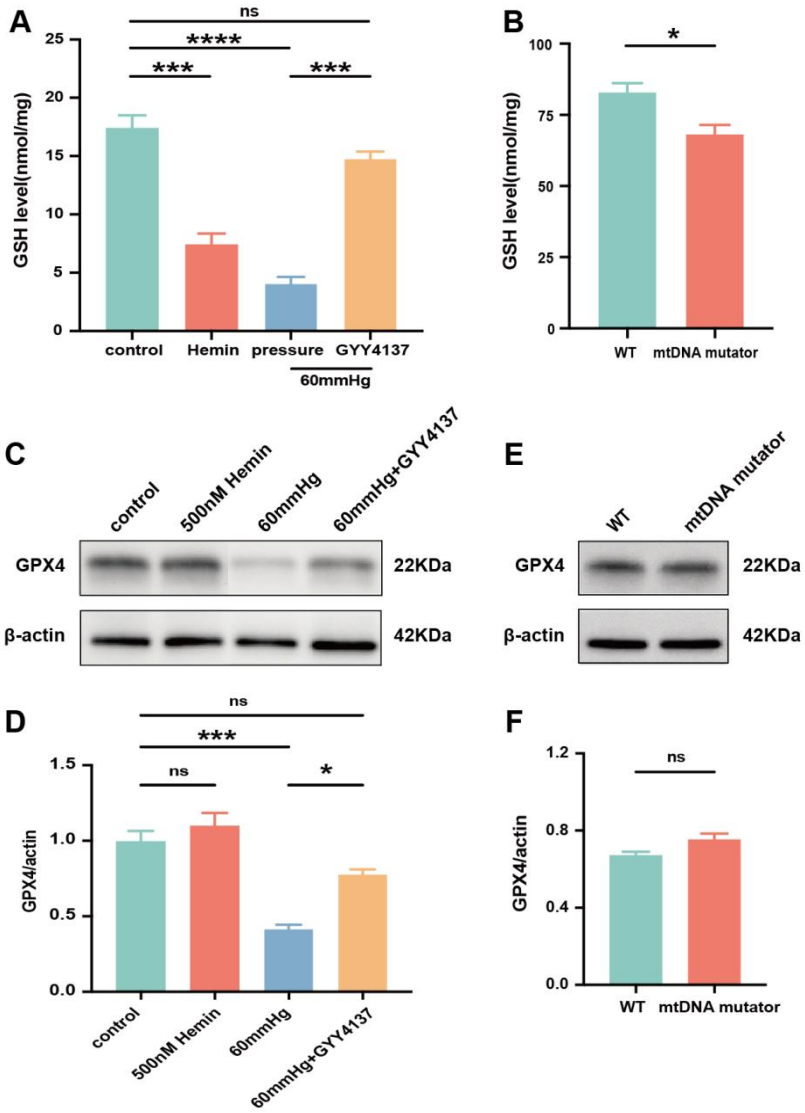

Figure 8 *(A) Quantification of GSH level in the retina. (B) Quantification of GSH level in the brains of mtDNA mutant mice and WT mice. (C, D) Western blot quantification of retinal GPx4 levels under iron overload and elevated hydrostatic pressure in culture. (E, F) Western blot quantification of GPx4 levels in brain of mtDNA mutant mice and WT mice.*

5.8. Elevated Hydrostatic Pressure Did Not Inhibit GPx4 Activity in NOX2$^{-/-}$ Mice Retina.

To further explore the relationship between NOX2 and retinal ferroptosis induced by elevated pressure. GPx4 expression in the retina of NOX2 knockout mice was detected. In NOX2 knockout mice, the expression of GPx4 was not affected in the retina under elevated hydrostatic pressure, as depicted in Figure 9.

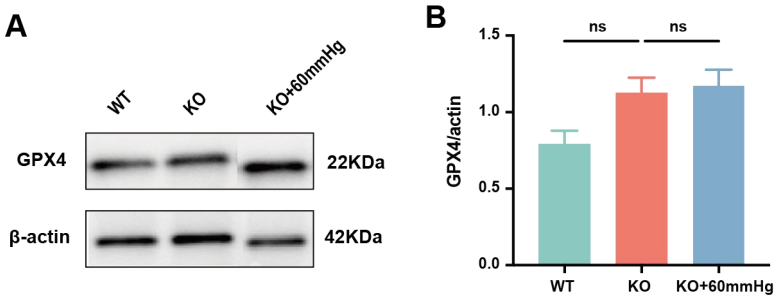

Figure 9 *Western blotting detection of GPx4 levels in retina of NOX2 knockout mice and WT mice with or without elevated pressure.*

6. Discussion

Studying the pathogenesis of glaucoma has been a core area of research in ophthalmology. Irreversible damage and death of the RGCs lead to optic nerve damage and visual field loss in glaucoma [5]. Pathologically elevated IOP is frequently considered the cause of RGCs death [6]. However, managing IOP alone does not safeguard against, so exploring the mechanism of RGCs death and reducing or delaying the loss of RGCs is crucial for developing clinical drugs for glaucoma. In this study, we explored the causes of RGCs death by either cauterizing the suprascleral vein of mice eyes to chronically elevate IOP for two weeks to mimic IOP elevation injury during glaucoma pathogenesis or by exposing retinal explants to elevated hydrostatic pressure in vitro.

Our investigation revealed significant alterations in pathways associated with iron homeostasis, mitochondrial dysfunction, and antioxidant defense mechanisms in an animal model experiencing chronic IOP elevation. Notably, both elevated pressure and mitochondrial dysfunction influenced iron levels and iron distribution within the retina and brain, rendering RGCs vulnerable to heightened concentrations of total and Fe^{2+}. We observed modifications in iron regulatory proteins attributed to elevated pressure, resulting in increased levels of free Fe^{2+} in the retina. Furthermore, augmented levels of Fe^{2+}, coupled with mitochondrial dysfunction, correlated with diminished antioxidant capacity, and increased ROS in the retina, although these conditions did not directly trigger ferroptosis. Conversely, pressure-induced injury alone demonstrated a notable association with increased ferroptosis. Notably, NOX2 emerged as a key upstream initiator of ferroptosis. Remarkably, pharmacological inhibition of NOX2 using H_2S or genetic knockout of NOX2 effectively attenuated pressure-induced ferroptosis in the retina.

6.1. The Interplay between Elevated Pressure, Mitochondrial Dysfunction, and Iron Homeostasis in Retina.

In our prior investigation, we delineated the disruption of pathways associated with iron regulation, ROS scavenging, mitochondrial homeostasis and function, and retinal vascular function due to acutely elevated IOP [20]. In this study, we validated the alteration of pathways linked to iron homeostasis, mitochondrial function, and antioxidant defense in a chronic IOP elevation animal model in vivo. These findings are consistent with results obtained from proteomic analyses of aqueous humor and serum collected from patients diagnosed with primary angle-closure glaucoma[25, 58].

Under normal physiological conditions, retinal iron levels are meticulously regulated [28]. Excessive iron can induce cytotoxic effects, while insufficient levels may lead to cellular dysfunction [59]. Therefore, maintaining retinal iron homeostasis is crucial for proper retinal function. Previous investigations have revealed that excessive iron assists to neuronal cell death in various neurodegenerative diseases [23-25]. However, the impact of excessive iron RGCs remains unclear. Our experiments unveiled the vulnerability of RGCs to iron overload, characterized by elevated levels of total iron and Fe^{2+}. Both elevated hydrostatic pressure and mitochondrial dysfunction were recognized as factors impacting total iron levels, Fe^{2+} levels, and iron composition in the retina and brain, respectively. While both high-pressure injury and mitochondrial dysfunction led to increased total iron and Fe^{2+} levels in the tissue, high-pressure injury resulted in an increased percentage of Fe^{2+} in the retina, whereas mitochondrial dysfunction led to a reduced percentage of Fe^{2+} in the brain. This suggested that mitochondrial dysfunction only partially contributed to the high-pressure-induced aberrant iron metabolism.

6.2. The Alterations in Iron Regulatory Proteins Following High-pressure Injury.

Iron metabolism is intricately regulated, focusing on import, export, and storage. We examined these aspects to uncover potential drivers of abnormal aberrant iron metabolism after pressure induced RGCs loss.

In the retina, TfR primarily mediates cellular iron uptake [60]. Fe^{3+} in the bloodstream adheres to transferrin, interacts with TfR on the cell membrane, and is incorporated via endocytosis [53]. Our investigation revealed that elevated hydrostatic pressure prompted an upregulation of TfR expression in the retina, suggesting an augmented capacity for inner retinal iron import.

Retinal iron export is mainly mediated by ferroportin, expressed in layers including the retinal GCL, IPL, INL, photoreceptor cell layer, and pigment epithelium layer [53]. Hepcidin, a key hormone in iron homeostasis, modulates ferroportin activity by inducing its degradation, thereby limiting cellular iron export [54, 61]. We observed increased Hepcidin expression in the retina following elevated hydrostatic pressure, leading to inhibited retinal iron export.

Ferritin, the principal iron storage protein, maintains iron balance by FTH1 and FTL [62]. Notably, our study found no significant alteration in FTH1 and FTL expression in the retina following high-pressure injury.

In summary, complex changes were observed in iron regulatory proteins in response to pressure conditions, characterized by marked enhancements in iron import and concomitant decreases in iron export. This observation aligns with the discovery of increased retinal iron content following high-pressure injury. Notably, while no significant changes were observed in iron storage proteins, this may be attributed to the expulsion of iron originally bound to ferritin into the cytoplasm. This corresponded with the notable increase in retinal free Fe^{2+} content observed under elevated hydrostatic pressure.

6.3. The Interconnection of Free Ferrous Iron, Mitochondrial Dysfunction, Antioxidant Capacity, and Ferroptosis.

Iron accumulation is a hallmark of various neurodegenerative diseases [27]. Our study found a substantial increase in total iron content and Fe^{2+} content in the retina after high-pressure injury. Moreover, Fe^{2+}, a potent oxidizing agent, generates hydroxyl radicals via the Fenton reaction and Haber-Weiss reaction [63]. These highly reactive hydroxyl radicals can oxidize lipid metabolites, particularly polyunsaturated fatty acids, forming cytotoxic lipid peroxides [64]. We found that both elevated hydrostatic pressure and iron overload lead to increased ROS and decreased GSH levels in the retina. Additionally, mitochondrial dysfunction also contributed to reduced GSH levels in the brain. However, the mechanisms underlying iron-mediated neurodegeneration seem to be more intricate than mere oxidative damage caused by iron [27].

Ferroptosis, a recently characterized form of iron-mediated cell death, typically involves substantial accumulation of Fe^{2+} and lipid peroxidation. Factors that induce iron toxicity affect glutathione peroxidase, leading to a diminution in cellular antioxidant capacity and accumulation of lipid ROS, ultimately giving rise to oxidative cell death [65]. GPx4 is a glutathione peroxidase whose main role is to neutralize harmful peroxides, and it also serves as an important regulator of ferroptosis [66, 67]. When intracellular levels of lethal lipid peroxides exceed the scavenging range of GPx4, this leads to the development of iron metabolism [29]. Our research found that both accumulation of iron and mitochondrial dysfunction resulted in reduced GSH levels, yet the reduction in GPx4 expression was observed solely triggered by elevated hydrostatic pressure. These results suggested that Fe^{2+} accumulation and mitochondrial dysfunction contributed solely to reduced antioxidant capacity. Although iron accumulation and mitochondrial dysfunction are pivotal to ferroptosis, these two factors alone are not sufficient to trigger ferroptosis. Instead, an additional upstream initiator of ferroptosis appears to be activated by high pressure.

6.4. NOX2, An Upstream Initiating Factor of Ferroptosis.

Iron also collaborates with ROS-producing enzymes such as NADPH oxidases, increasing intracellular ROS production [26, 63]. Our study highlighted a growth in NOX2 expression in the retina under elevated hydrostatic pressure, whereas iron overload did not affect NOX2 expression. These suggested a potential correlation between NOX2 and ferroptosis in retina.

To substantiate the association between NOX2 and ferroptosis, we exposed retinas from NOX2 knockout mice to elevated hydrostatic pressure. Intriguingly, the absence of NOX2 had no considerable impact on the expression of GPx4 in the retina following high-pressure injury. This underscores the role of NOX2 as a principal upstream initiator regulating high-pressure-induced ferroptosis.

6.5. Pharmacological Intervention with H_2S

In our previous study, we observed that endogenous H_2S synthase was elevated in glaucoma animal models after IOP elevation [20]. Additionally, we demonstrated that the slow-releasing H_2S precursor significantly enhanced the survival of RGCs in various in vitro and in vivo glaucoma models [41]. Subsequently, we discovered that exogenous H_2S showed its neuroprotective effects in an acute IOP elevation animal model by modulating pathways related to iron metabolism, ROS clearance, mitochondrial homeostasis and function, and maintenance of retinal vascular function [20]. In this study, based on analyzing the particular function of iron homeostasis in glaucoma pathogenesis, we illustrated the protective effect of H_2S in more detail and furthered our understanding of its neuroprotective potential.

Our findings demonstrated the protective role of H_2S against the loss of RGCs induced by high pressure, functioning as an iron chelator. This is because its sulfide ions can readily bind with free iron radicals, effectively chelating Fe^{2+} [68]. It is noteworthy that H_2S is considered a physiological gas transmitter, with its importance comparable to that of nitric oxide and carbon monoxide, possessing neuroprotective properties that transcend its chemical characteristics [31]. Our results further revealed the impact of H_2S on iron regulatory proteins, thereby reducing total iron content under high-pressure injury. Coupled with its chelation of free Fe^{2+}, it significantly contributed to the replenishment of GSH levels and reduction of ROS production. Moreover, H_2S exerts its protective effects by inhibiting NOX2, thereby alleviating ferroptosis induced by high pressure.

6.6. Conclusion

This study reveals the pathological mechanisms underlying RGCs loss induced by high pressure. We emphasize that disrupted iron homeostasis, mitochondrial dysfunction, and antioxidant defense mechanisms play significant roles in pressure induced RGCs injury. Following high-pressure injury, there is an elevation in total iron content, free ferrous iron, and NOX2 in the retina, leading to increased generation of ROS, diminished antioxidant capacity, and induction of ferroptosis in the retina. While iron accumulation and mitochondrial dysfunction play pivotal roles in ferroptosis, they are inadequate as the sole triggers for this process. Ferroptosis is primarily instigated by heightened NOX2 activity. Knockdown of NOX2 and pharmacological inhibition of NOX2 with H_2S effectively alleviate pressure-induced ferroptosis, concurrently reducing ROS production and enhancing RGCs survival rates. Additionally, H_2S stabilizes iron homeostasis, chelating excessive ferrous iron in the retina, thus protecting RGCs from pressure-induced damage (Figure 10).

These findings indicate that NOX2 is a groundbreaking target for glaucoma treatment. Due to the multifactorial nature of glaucoma pathogenesis, effective therapeutic interventions targeting multiple pathways are essential. Our findings further clarify the multiple mechanisms by which H_2S acts as a neuroprotective agent. Slow-releasing H_2S precursor may be promising therapeutic agents for mitigating RGCs damage in glaucoma.

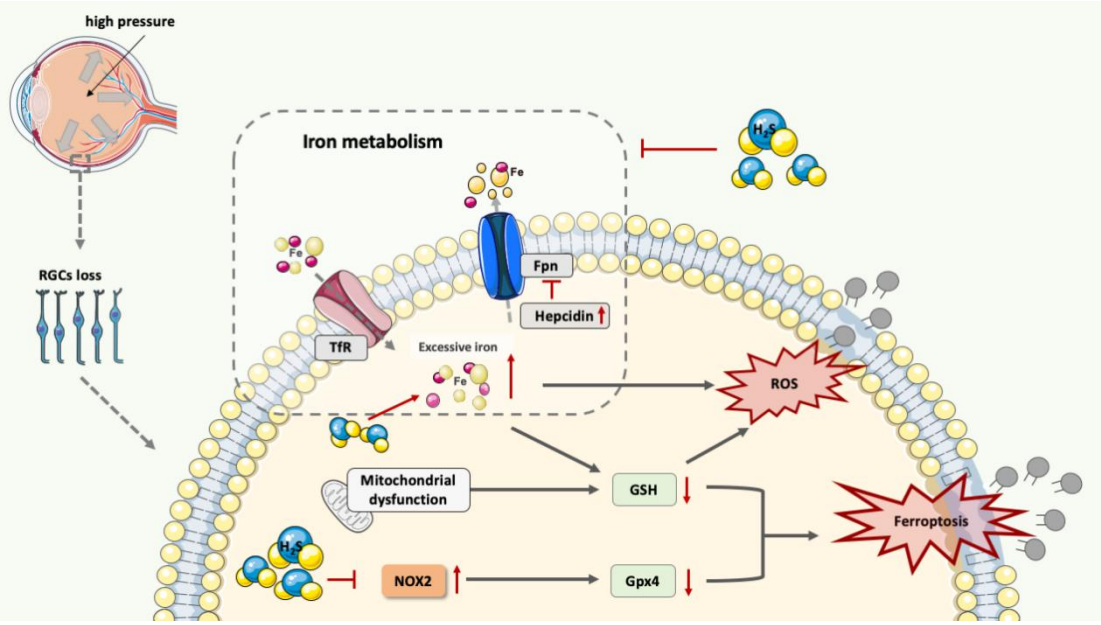

Figure 10 Potential mechanisms of high pressure induced RGCs loss and the multifaceted roles of H_2S.

Elevated intraocular pressure induces alterations in iron metabolism and mitochondrial function. High pressure increases iron import, reduces iron export, and results in increased retinal free ferrous iron content. The elevation in iron content leads to the generation of ROS.

Both the increased iron content and mitochondrial dysfunction contribute to a reduction in antioxidant capacity, yet they do not induce ferroptosis directly. Ferroptosis primarily occurs when NOX2 activity is heightened. H_2S acts by chelating free radical iron and reducing Fe^{2+} levels. It also impacts iron regulatory proteins, alleviating the increase in total iron content induced by elevated pressure in the retina. Its dual action in regulating iron metabolism contributes to the restoration of GSH levels and reduction in ROS production. Additionally, H_2S shows its protective effect by inhibiting NOX2, thereby safeguarding RGCs against high-pressure-induced ferroptosis.

7. Reference

1. Jonas, J.B., et al., Glaucoma. Lancet, 2017. 390(10108): p. 2183-2193.
2. Kang, J.M. and A.P. Tanna, Glaucoma. Med Clin North Am, 2021. 105(3): p. 493-510.
3. Martersteck, E.M., et al., Diverse Central Projection Patterns of Retinal Ganglion Cells. Cell Rep, 2017. 18(8): p. 2058-2072.
4. Kay, J.N., et al., Retinal ganglion cells with distinct directional preferences differ in molecular identity, structure, and central projections. J Neurosci, 2011. 31(21): p. 7753-62.
5. Cohen, L.P. and L.R. Pasquale, Clinical characteristics and current treatment of glaucoma. Cold Spring Harb Perspect Med, 2014. 4(6).
6. Qu, J., D. Wang, and C.L. Grosskreutz, Mechanisms of retinal ganglion cell injury and defense in glaucoma. Exp Eye Res, 2010. 91(1): p. 48-53.
7. Stiemke, A.B., et al., Systems Genetics of Optic Nerve Axon Necrosis During Glaucoma. Front Genet, 2020. 11: p. 31.
8. Weinreb, R.N., T. Aung, and F.A. Medeiros, The pathophysiology and treatment of glaucoma: a review. JAMA, 2014. 311(18): p. 1901-11.
9. Erichev, V.P., G.K. Khachatryan, and O.V. Khomchik, [Current trends in studying pathogenesis of glaucoma]. Vestn Oftalmol, 2021. 137(5. Vyp. 2): p. 268-274.
10. Mursch-Edlmayr, A.S., M. Bolz, and C. Strohmaier, Vascular Aspects in Glaucoma: From Pathogenesis to Therapeutic Approaches. Int J Mol Sci, 2021. 22(9).
11. Storgaard, L., et al., Glaucoma Clinical Research: Trends in Treatment Strategies and Drug Development. Front Med (Lausanne), 2021. 8: p. 733080.
12. Chang, E.E. and J.L. Goldberg, Glaucoma 2.0: neuroprotection, neuroregeneration, neuroenhancement. Ophthalmology, 2012. 119(5): p. 979-86.
13. Joshi, P., et al., Glaucoma in Adults-diagnosis, Management, and Prediagnosis to End-stage, Categorizing Glaucoma's Stages: A Review. J Curr Glaucoma Pract, 2022. 16(3): p. 170-178.
14. Pascale, A., F. Drago, and S. Govoni, Protecting the retinal neurons from glaucoma: lowering ocular pressure is not enough. Pharmacological Research, 2012. 66(1): p. 19-32.
15. Dutt, S., I. Hamza, and T.B. Bartnikas, Molecular Mechanisms of Iron and Heme Metabolism. Annu Rev Nutr, 2022. 42: p. 311-335.
16. He, X., et al., Iron homeostasis and toxicity in retinal degeneration. Prog Retin Eye Res, 2007. 26(6): p. 649-73.
17. Ramdas, W.D., The relation between dietary intake and glaucoma: a systematic review. Acta Ophthalmol, 2018. 96(6): p. 550-556.
18. Wang, S.Y., K. Singh, and S.C. Lin, The association between glaucoma prevalence

and supplementation with the oxidants calcium and iron. Invest Ophthalmol Vis Sci, 2012. 53(2): p. 725-31.

19. Yao, F., et al., Pathologically high intraocular pressure disturbs normal iron homeostasis and leads to retinal ganglion cell ferroptosis in glaucoma. Cell Death Differ, 2022.
20. Liu, H., et al., Proteomics Reveals the Potential Protective Mechanism of Hydrogen Sulfide on Retinal Ganglion Cells in an Ischemia/Reperfusion Injury Animal Model. Pharmaceuticals (Basel), 2020. 13(9).
21. Huang, S., et al., Research progress of ferroptosis in glaucoma and optic nerve damage. Mol Cell Biochem, 2023. 478(4): p. 721-727.
22. Basavarajappa, D., et al., Signalling pathways and cell death mechanisms in glaucoma: Insights into the molecular pathophysiology. Mol Aspects Med, 2023. 94: p. 101216.
23. Ashraf, A., et al., Iron dyshomeostasis, lipid peroxidation and perturbed expression of cystine/glutamate antiporter in Alzheimer's disease: Evidence of ferroptosis. Redox Biol, 2020. 32: p. 101494.
24. Belaidi, A.A. and A.I. Bush, Iron neurochemistry in Alzheimer's disease and Parkinson's disease: targets for therapeutics. J Neurochem, 2016. 139 Suppl 1: p. 179-197.
25. Mahad, D.H., B.D. Trapp, and H. Lassmann, Pathological mechanisms in progressive multiple sclerosis. Lancet Neurol, 2015. 14(2): p. 183-93.
26. Dixon, S.J., et al., Ferroptosis: an iron-dependent form of nonapoptotic cell death. Cell, 2012. 149(5): p. 1060-72.
27. Masaldan, S., et al., Striking while the iron is hot: Iron metabolism and ferroptosis in neurodegeneration. Free Radic Biol Med, 2019. 133: p. 221-233.
28. Aisen, P., C. Enns, and M. Wessling-Resnick, Chemistry and biology of eukaryotic iron metabolism. Int J Biochem Cell Biol, 2001. 33(10): p. 940-59.
29. Ursini, F. and M. Maiorino, Lipid peroxidation and ferroptosis: The role of GSH and GPx4. Free Radic Biol Med, 2020. 152: p. 175-185.
30. Osborne, N.N., et al., Glutamate oxidative injury to RGC-5 cells in culture is necrostatin sensitive and blunted by a hydrogen sulfide (H2S)-releasing derivative of aspirin (ACS14). Neurochem Int, 2012. 60(4): p. 365-78.
31. Paul, B.D. and S.H. Snyder, Gasotransmitter hydrogen sulfide signaling in neuronal health and disease. Biochem Pharmacol, 2018. 149: p. 101-109.
32. Wang, R., Two's company, three's a crowd: can H2S be the third endogenous gaseous transmitter? FASEB J, 2002. 16(13): p. 1792-8.
33. Chen, C.Q., H. Xin, and Y.Z. Zhu, Hydrogen sulfide: third gaseous transmitter, but

with great pharmacological potential. Acta Pharmacol Sin, 2007. 28(11): p. 1709-16.
34. Picard, E., et al., From Rust to Quantum Biology: The Role of Iron in Retina Physiopathology. Cells, 2020. 9(3).
35. Kimura, Y. and H. Kimura, Hydrogen sulfide protects neurons from oxidative stress. FASEB J, 2004. 18(10): p. 1165-7.
36. Kimura, Y., Y. Goto, and H. Kimura, Hydrogen sulfide increases glutathione production and suppresses oxidative stress in mitochondria. Antioxid Redox Signal, 2010. 12(1): p. 1-13.
37. Lv, B., et al., Hydrogen sulfide and vascular regulation - An update. J Adv Res, 2021. 27: p. 85-97.
38. Tabassum, R. and N.Y. Jeong, Potential for therapeutic use of hydrogen sulfide in oxidative stress-induced neurodegenerative diseases. Int J Med Sci, 2019. 16(10): p. 1386-1396.
39. Giovinazzo, D., et al., Hydrogen sulfide is neuroprotective in Alzheimer's disease by sulfhydrating GSK3beta and inhibiting Tau hyperphosphorylation. Proc Natl Acad Sci U S A, 2021. 118(4).
40. Tabassum, R., N.Y. Jeong, and J. Jung, Therapeutic importance of hydrogen sulfide in age-associated neurodegenerative diseases. Neural Regen Res, 2020. 15(4): p. 653-662.
41. Liu, H., et al., Hydrogen Sulfide Protects Retinal Ganglion Cells Against Glaucomatous Injury In Vitro and In Vivo. Invest Ophthalmol Vis Sci, 2017. 58(12): p. 5129-5141.
42. Trifunovic, A., et al., Premature ageing in mice expressing defective mitochondrial DNA polymerase. Nature, 2004. 429(6990): p. 417-23.
43. Wang, M., et al., Intraocular Pressure-Induced Endothelial Dysfunction of Retinal Blood Vessels Is Persistent, but Does Not Trigger Retinal Ganglion Cell Loss. Antioxidants (Basel), 2022. 11(10).
44. Owen, J.E., G.M. Bishop, and S.R. Robinson, Uptake and Toxicity of Hemin and Iron in Cultured Mouse Astrocytes. Neurochem Res, 2016. 41(1-2): p. 298-306.
45. Seiwert, N., et al., Heme oxygenase 1 protects human colonocytes against ROS formation, oxidative DNA damage and cytotoxicity induced by heme iron, but not inorganic iron. Cell Death Dis, 2020. 11(9): p. 787.
46. Joly, S., et al., Human beta-defensins 2 and 3 demonstrate strain-selective activity against oral microorganisms. J Clin Microbiol, 2004. 42(3): p. 1024-9.
47. Nin, D.S., et al., Biological Effects of Morpholin-4-Ium 4 Methoxyphenyl (Morpholino) Phosphinodithioate and Other Phosphorothioate-Based Hydrogen Sulfide Donors. Antioxid Redox Signal, 2020. 32(2): p. 145-158.

48. Hughes, C.S., et al., Single-pot, solid-phase-enhanced sample preparation for proteomics experiments. Nat Protoc, 2019. 14(1): p. 68-85.
49. Braun, F., et al., The proteomic landscape of small urinary extracellular vesicles during kidney transplantation. J Extracell Vesicles, 2020. 10(1): p. e12026.
50. Nadal-Nicolás, F.M., et al., Brn3a as a marker of retinal ganglion cells: qualitative and quantitative time course studies in naive and optic nerve-injured retinas. Investigative Ophthalmology & Visual Science, 2009. 50(8): p. 3860-3868.
51. Noctor, G., et al., Glutathione. Arabidopsis Book, 2011. 9: p. e0142.
52. Gericke, A., et al., Elevated Intraocular Pressure Causes Abnormal Reactivity of Mouse Retinal Arterioles. Oxid Med Cell Longev, 2019. 2019: p. 9736047.
53. Gnana-Prakasam, J.P., et al., Expression and function of iron-regulatory proteins in retina. IUBMB Life, 2010. 62(5): p. 363-70.
54. Gnana-Prakasam, J.P., et al., Hepcidin expression in mouse retina and its regulation via lipopolysaccharide/Toll-like receptor-4 pathway independent of Hfe. Biochem J, 2008. 411(1): p. 79-88.
55. Kajarabille, N. and G.O. Latunde-Dada, Programmed Cell-Death by Ferroptosis: Antioxidants as Mitigators. Int J Mol Sci, 2019. 20(19).
56. Noreng, S., et al., Structure of the core human NADPH oxidase NOX2. Nat Commun, 2022. 13(1): p. 6079.
57. Yang, W.S., et al., Regulation of ferroptotic cancer cell death by GPX4. Cell, 2014. 156(1-2): p. 317-331.
58. Liu, X., et al., Proteome Characterization of Glaucoma Aqueous Humor. Mol Cell Proteomics, 2021. 20: p. 100117.
59. Sung, H.K., et al., Autophagy deficiency exacerbates iron overload induced reactive oxygen species production and apoptotic cell death in skeletal muscle cells. Cell Death Dis, 2023. 14(4): p. 252.
60. Petit, F., et al., Defective palmitoylation of transferrin receptor triggers iron overload in Friedreich ataxia fibroblasts. Blood, 2021. 137(15): p. 2090-2102.
61. Theurl, M., et al., Mice with hepcidin-resistant ferroportin accumulate iron in the retina. FASEB J, 2016. 30(2): p. 813-23.
62. Muhoberac, B.B. and R. Vidal, Iron, Ferritin, Hereditary Ferritinopathy, and Neurodegeneration. Front Neurosci, 2019. 13: p. 1195.
63. Dixon, S.J. and B.R. Stockwell, The role of iron and reactive oxygen species in cell death. Nat Chem Biol, 2014. 10(1): p. 9-17.
64. Barrera, G., Oxidative stress and lipid peroxidation products in cancer progression and therapy. ISRN Oncol, 2012. 2012: p. 137289.
65. Li, J., et al., Ferroptosis: past, present and future. Cell Death Dis, 2020. 11(2): p. 88.

66. Ma, T., et al., GPX4-independent ferroptosis-a new strategy in disease's therapy. Cell Death Discov, 2022. 8(1): p. 434.
67. Gaschler, M.M., et al., FINO(2) initiates ferroptosis through GPX4 inactivation and iron oxidation. Nat Chem Biol, 2018. 14(5): p. 507-515.
68. Pal, V.K., P. Bandyopadhyay, and A. Singh, Hydrogen sulfide in physiology and pathogenesis of bacteria and viruses. IUBMB Life, 2018. 70(5): p. 393-410.

8. Appendix

Supplementary Data S1: Impact of Different Concentrations of Hemin on RGCs

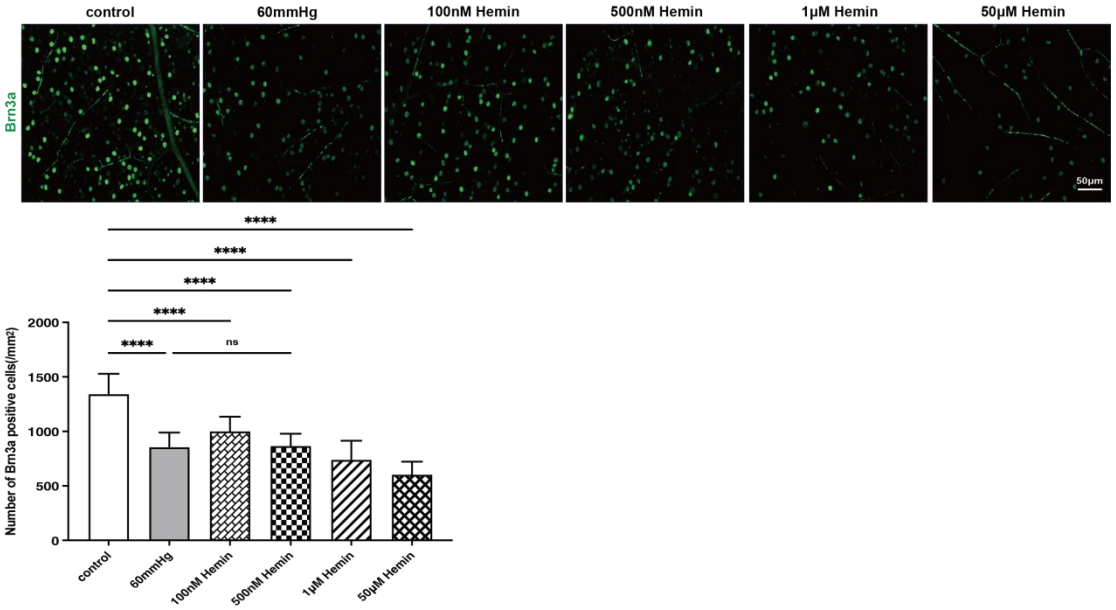

Figure S1 *Representative fluorescence microscopy of Brn3a staining in different Hemin concentrations. At 500 nMHemin, RGCs loss was like that induced by high pressure. (scale bar = 50 μm)*